BJR

INFECTION

Treatment of osteomyelitis defects by a vancomycin-loaded gelatin/β-tricalcium phosphate composite scaffold

J. Zhou,
X. G. Zhou,
J. W. Wang,
H. Zhou,
J. Dong

Zhongshan Hospital, Fudan University, Shanghai 200032, China

Objective

In the present study, we aimed to assess whether gelatin/β-tricalcium phosphate (β-TCP) composite porous scaffolds could be used as a local controlled release system for vancomycin. We also investigated the efficiency of the scaffolds in eliminating infections and repairing osteomyelitis defects in rabbits.

Methods

The gelatin scaffolds containing differing amounts of of β-TCP (0%, 10%, 30% and 50%) were prepared for controlled release of vancomycin and were labelled G-TCP0, G-TCP1, G-TCP3 and G-TCP5, respectively. The Kirby-Bauer method was used to examine the release profile. Chronic osteomyelitis models of rabbits were established. After thorough debridement, the osteomyelitis defects were implanted with the scaffolds. Radiographs and histological examinations were carried out to investigate the efficiency of eliminating infections and repairing bone defects.

Results

The prepared gelatin/β-TCP scaffolds exhibited a homogeneously interconnected 3D porous structure. The G-TCP0 scaffold exhibited the longest duration of vancomycin release with a release duration of eight weeks. With the increase of β-TCP contents, the release duration of the β-TCP-containing composite scaffolds was decreased. The complete release of vancomycin from the G-TCP5 scaffold was achieved within three weeks. In the treatment of osteomyelitis defects in rabbits, the G-TCP3 scaffold showed the most efficacious performance in eliminating infections and repairing bone defects.

Conclusions

The composite scaffolds could achieve local therapeutic drug levels over an extended duration. The G-TCP3 scaffold possessed the optimal porosity, interconnection and controlled release performance. Therefore, this scaffold could potentially be used in the treatment of chronic osteomyelitis defects.

Cite this article: *Bone Joint Res* 2018;7:46–57.

Keywords: Composite porous scaffold, Vancomycin, Osteomyelitis defect

Article focus

- To assess whether gelatin/β-TCP composite porous scaffolds could be used as a controlled local release system for vancomycin.
- To investigate the scaffold efficiency in eliminating infections and repairing osteomyelitis defects in rabbits.

Key messages

- The desired local therapeutic drug levels could be achieved by gelatin/β-TCP composite scaffolds over an extended duration.
- The composite scaffold consisting of gelatin and 30% β-TCP granules showed optimal porosity, interconnection and controlled release performances. It exhibited good performances in infection control and bone defect repair in the chronic methicillin-resistant *Staphylococcus aureus* osteomyelitis model.

Strengths and limitations

- Additional studies with larger animals such as sheep are necessary to confirm

J. Zhou, MD, Orthopaedic Surgeon,
X. G. Zhou, MD, Orthopaedic Surgeon,
J. W. Wang, MD, Orthopaedic Surgeon,
H. Zhou, MD, Orthopaedic Surgeon,
J. Dong, MD, PhD, Orthopaedic Surgeon, Department of Orthopaedic Surgery, Zhongshan Hospital, Fudan University, Shanghai 200032, China.

Correspondence should be sent to J. Dong; email: dong.jian@zs-hospital.sh.cn

doi: 10.1302/2046-3758.71.BJR-2017-0129.R2

Bone Joint Res 2018;7:46–57.

whether the vancomycin-loaded gelatin/β-TCP composite scaffold could potentially be used in the clinical treatment of osteomyelitis defects.

Introduction

Despite modern advances in antibiotics and surgical techniques, osteomyelitis, especially methicillin-resistant *Staphylococcus aureus* (MRSA) osteomyelitis, remains a serious challenge to orthopaedic surgeons. It is difficult to concurrently repair bone and inhibit infection. The mainstay of treatment for osteomyelitis is a combination of multiple surgical debridements and systemic antibiotic therapy followed by bone grafting.[1]

The successful treatment of this disease involves adequate debridement of all involved soft tissue and bone until only viable bleeding tissue remains. Inadequate debridement to preserve the structural integrity of the bone leads to the recurrence of infection.[2] However, intensive debridement may leave a huge cavity in the local tissue. Bone grafting for primary repair is often associated with high failure rates and bone reinfection.[3] On the other hand, long-term treatment with systemic antibiotics is expensive, prone to complications and can result in unsuccessful repair. Only a small fraction of a given dose reaches the site of infection and high systemic levels of antibiotics are associated with a high incidence of nephrotoxicity, ototoxicity and gastrointestinal side effects.

In contrast to treatment with systemic antibiotics, local delivery systems can achieve a sustained high concentration of antibiotics at the contaminated site, resulting in a more effective treatment of the infection, as well as reduced systemic toxicity concerns.[4] Polymethyl methacrylate (PMMA) cement beads have become the most widely studied and applied local antibiotic delivery system and were first introduced by Buchholz et al.[5] PMMA beads have been found to be successful for the treatment and prevention of osseous infections, representing the current benchmark for local antibiotic delivery in clinical studies.[4,6] However, PMMA is a non-biodegradable material, and the disadvantages associated with the PMMA beads include a secondary surgical procedure for bead removal and an incomplete and very slow drug release. Furthermore, the cavity may require reconstruction after the bead removal. Therefore, it is necessary to control local antibiotic release from biodegradable materials and simultaneously promote bone regeneration to avoid multiple surgeries and delayed reconstruction. These biodegradable materials should have certain characteristics, such as improved tissue compatibility, no negative effects on osteogenesis *in vivo* and the ability to control the release rate of antibiotics.

As a complex material, bone is composed of calcium phosphate deposited within an organic matrix mainly consisting of type I collagen. Gelatin is a natural polymer obtained by physicochemical degradation of collagen. Unlike more common proteins, gelatin does not exhibit antigenicity and is completely bioresorbable in biological environments. Gelatin has been extensively used for pharmaceutical and medical purposes because of its biodegradability and biocompatibility in physiological environments. Various gelatin-based controlled-release systems can be achieved depending on the fabrication method.[7-9] However, the gelatin-based scaffolds generally exhibit a narrow and limited range of mechanical properties which limit their biomedical application. On the other hand, the modern biomaterials for orthopaedic applications must not only be biocompatible and bioresorbable, but also osteoconductive. To overcome these drawbacks, composite scaffolds with ceramics have been prepared; the ceramic phase in polymer composites is important for improving the mechanical and osteoconductive properties of scaffolds.[10-12]

Calcium phosphate ceramics, such as hydroxyapatite (HA) and β-tricalcium phosphate (β-TCP), are excellent candidates for bone repair and regeneration because their chemical compositions are very similar to the inorganic components of bone.[13] However, HA cannot be degraded under physical conditions. Beta-TCP has been shown to be bioactive and is also biodegradable. The degradation rate of β-TCP is ten times higher than that of HA.[14] It has been demonstrated by some researchers that the gelatin/β-TCP composite scaffold is suitable for repairing bone defects. The composite scaffold exhibits better osteoconduction and can be progressively replaced by newly formed bone to accomplish bone defect repair.[15,16] Our previous work has shown that a biodegradable gelatin sponge containing different amounts of β-TCP can control the release of vancomycin.[17] However, further studies are still required to evaluate the therapeutic effects of vancomycin-loaded gelatin/β-TCP composite scaffolds on the treatment of osteomyelitis.

In the present study, we aimed to investigate whether vancomycin-loaded composite scaffolds could effectively eliminate infections and repair bone defects in an animal model. The vancomycin-loaded composite scaffolds containing differing amounts of β-TCP were prepared and implanted to treat osteomyelitis defects in rabbits. Taken together, our findings provide an experimental basis for the clinical application of vancomycin-loaded composite scaffolds in the treatment of osteomyelitis defects.

Materials and Methods

All animals were provided by the Laboratory Animal Center of Zhongshan Hospital. All procedures were performed at the Animal Center with approval from the Zhongshan Hospital Animal Care and Use Committee.

Preparation of vancomycin-loaded gelatin/β-TCP composite scaffolds. The scaffolds were prepared by a previously reported freeze-casting method with minor modifications.[18] Scaffolds were typically obtained as follows: briefly, a gelatin aqueous solution of 16.67 weight% was

prepared by dissolving 2.5 g of gelatin powder Type A, G-2500, approximately 300 Bloom, (Sigma-Aldrich, St. Louis, Missouri) into 15 mL of deionized water at 50°C with stirring for one hour. Subsequently, different amounts of β-TCP (0 g, 0.25 g, 0.75 g and 1.25 g) were added to 15 mL of gelatin solution at 37°C to obtain suspensions with different compositions. The ratios between β-TCP and gelatin (weight/weight %) were 0:10, 1:10, 3:10 and 5:10. After constant stirring for 45 minutes, 2 mL aqueous solution containing 250 mg of vancomycin (one-tenth of the total amount of gelatin) and 8 mL aqueous solution containing 0.234 g of gelatin (one-64th of the total amount of gelatin) were added to the gelatin/β-TCP composite solution. After the crosslinking reaction was carried out at room temperature for 48 hours, the crosslinked gelatin hydrogels were frozen at -20℃ for 24 hours and then freeze-dried. The composite scaffolds were labelled according to their contents in the inorganic phase as follows: G-TCP0 (the weight ratio between β-TCP and gelatin was 0:10), G-TCP1(the weight ratio between β-TCP and gelatin was 1:10), G-TCP3 (the weight ratio between β-TCP and gelatin was 3:10) and G-TCP5 (the weight ratio between β-TCP and gelatin was 5:10). The acquired scaffolds were then sputter-coated with gold and the morphology was examined under a scanning electron microscope (SEM), JSM-5600, (JEOL CO. LTD, Tokyo, Japan). The mean pore size of the scaffolds was evaluated by geometrical measurements on the scanning electron micrographs, and the porosity of the composite scaffold was measured by the method reported previously.[19] In brief, the porosity of the pure gelatin scaffold, εgelatin, was calculated from its apparent density, ρ*gelatin, and the density of gelatin, ρgelatin (1.25 g/cm^3), by the following equation: εgelatin = 1 –ρ*gelatin/ρgelatin, where ρ*gelatin was determined by measuring the weight and volume of a cubic pure gelatin scaffold. The porosity of the gelatin/β-TCP composite scaffold, εC, was calculated by the following equation: εC = εgelatin – ρ*C/ρC, where ρC was the density of β-TCP (3.14 g/cm^3) and ρ*C was the apparent density of the hybrid sponge which was derived from the weight and volume of the cubic hybrid sponge.

The release profile and antibacterial properties of vancomycin released from composite scaffolds. The release profile of vancomycin released from the composite scaffold was identified using the Kirby-Bauer (K-B) disc diffusion method.

The standard curve was first established to explore the optimal drug concentration by inputting the diameters of inhibition zones. Filter paper discs (diameter 8 mm) impregnated with 20 µL of serial vancomycin dilutions of known concentrations were aseptically placed on petri plates (Thermo Fisher Scientific Inc, Waltham, Massachusetts) containing Mueller-Hinton agar (Difco) (Thermo Fisher Scientific Inc,) and seeded with 10^8 colony-forming units (CFU)/mL (0.5 McFarland)[20] of *Staphylococcus epidermidis* strain RP62A and then the petri plates were incubated overnight. The diameters of the inhibition zones around the paper discs were determined with a micrometer. The correlation between zone sizes and vancomycin concentrations (150 µg/mL, 100 µg/mL, 80 µg/mL, 60 µg/mL, 40 µg/mL, 20 µg/mL and 10 µg/mL) were identified by constructing a standard curve. The zone diameter for each test sample was determined as a mean of six inhibition zones in two agar plates (three discs per plate). Regression analysis was performed with Microsoft Excel 2016 (Microsoft Corp., Redmond, Washington) to generate the final standard curve.

A total of 27 nine-week-old Sprague Dawley rats, each weighing 250 g to 300 g, were obtained, and each rat was implanted with one scaffold from each group, totaling four scaffolds per rat (G-TCP0, G-TCP1, G-TCP3 and G-TCP5). Before implantation, the gelatin/β-TCP composite scaffolds were cut into a cube (5 mm × 5 mm × 5 mm in size, the weight of each implant was approximately 30 mg) and sterilized with ethylene oxide. Chloral hydrate (Wako Pure Chemical Industries, Ltd, Hokkaidō, Japan) served as an anaesthetic agent (peritoneal injection, 3.0 mg/100 g body weight). Under sterile conditions, four muscular pouches were established on the back of each rat, where vancomycin-loaded scaffolds were implanted. At each of the designated timepoints (three days, seven days, ten days, 14 days, 21 days, 28 days, 35 days, 42 days and 56 days), three rats were sacrificed. An amount of 1.0 g of muscle specimen close to the implants (0.5cm apart around the center of the specimen) was collected and homogenized, and then the obtained homogenate was resuspended in 5 mL of physiological saline to measure the drug concentration by the K-B method as previously described.[21] Briefly, 20 µL of the homogenate was added onto filter paper discs in petri plates and incubated at 37°C overnight, and the inhibition zone of bacterial growth around the discs was analysed.

Preliminary biocompatibility. Intramuscular implantation is an important step to test *in vivo* biocompatibility and the degradation properties of a bioabsorbable polymer.[22] To evaluate the biocompatibility of the vancomycin-loaded composite scaffolds, the implants in each group, along with the surrounding tissues, were removed to investigate the tissue reaction, inflammation and degradation at each of three designated timepoints (two weeks, four weeks and eight weeks after implantation). The samples harvested at different timepoints were washed in phosphate-buffered saline (PBS) and fixed in 10% formalin solution. After dehydration through a graded series of alcohols, paraffin-embedded samples were cut into 5 µm sections. Sections were then deparaffinized, rehydrated through a graded series of alcohols and stained with haematoxylin and eosin (H&E) for histological observation.

Osteomyelitis model. A total of 43 New Zealand white rabbits (21 female, 22 male), each weighing 1.8 kg to 2.2 kg (approximately six months of age), were used for this study. The osteomyelitis model was established as previously described.[23] Briefly, anaesthesia was initiated by intravenously injecting 3% sodium pentobarbital (30 mg/kg). The right hind leg of the animals was shaved and disinfected with 2% iodine solution. After being draped with sterile sheets, a 12-gauge needle was percutaneously inserted into the medullary cavity from the lateral aspect of the proximal tibial metaphysis, and 0.3 mL bone marrow was extracted. Subsequently, 0.1 mL 5% morrhuate sodium and 0.1 mL MRSA (1×10^9 CFU/mL) were injected through the same needle. The needle was then flushed with 0.1 mL of 0.9% sodium chloride to ensure that all bacteria reached the tibial cavity. During the experiment, the animals were kept in individual cages, fed a routine diet and allowed to be fully active. The infection could progress for three weeks, during which the severity of osteomyelitis was radiologically determined.

The severity of osteomyelitis was confirmed by radiographs according to the descriptive criteria of Norden[24] at three weeks after the induction of osteomyelitis. These criteria are based on the presence of sequestra, periosteal new bone formation and destruction of bone. A numerical score was assigned to each variable. All scores were added to create a composite radiological score with a maximum of six, representing radiological severity. Two radiologists (JZ and HZ) blindly and independently evaluated these images. Three rabbits with signs of osteomyelitis on the radiograph were randomly selected and sacrificed. Gross examination and histological observation were performed to evaluate the presence of osteomyelitis.

Debridement and implantation of vancomycin-loaded composite scaffolds. The remaining 40 rabbits with radiological evidence of osteomyelitis underwent debridement at three weeks after the induction of osteomyelitis. A 3 cm incision was made over the lateral aspect of the proximal tibial metaphysis, parallel to the tibial shaft. The necrotic, hardening and infected soft and bone tissues were removed. After the infected soft and bone tissues were cleaned, the wounds were washed with 2% hydrogen peroxide solution and saline. After debridement, all of the rabbits were randomly distributed into four groups as follows: control group ($n = 4$) in which the rabbits were treated with debridement only ; G-TCP0 group ($n = 12$) in which the rabbits were treated with debridement and implanted with vancomycin-loaded G-TCP0 scaffold; G-TCP1 group ($n = 12$) in which the rabbits were treated with debridement and implanted with vancomycin-loaded G-TCP1 composite scaffold; and G-TCP3 group ($n = 12$) in which the rabbits were treated with debridement and implanted with vancomycin-loaded G-TCP3 composite scaffold. The rabbits of G-TCP0, G-TCP1 and G-TCP3 groups were implanted with the same amounts of the sterilized scaffolds (G-TCP0, G-TCP1 and G-TCP3, 1.0cm×0.5cm×0.5cm, respectively) in the defect site. After implantation, the incision was closed layer by layer.

Assessment of therapeutic efficacy: radiographic and histological evaluation. At the preset timepoints (four weeks and eight weeks after debridement), radiographic examination and histological observation of two rabbits from the control group and six rabbits from each of the other groups were conducted. After the rabbits were sacrificed, anteroposterior and lateral radiographs of their right tibias were taken at 50 kV, 100 mA and 12 ms. These images were also blindly and independently evaluated by two radiologists according to the criteria described by Norden[24] A numerical score was assigned to each variable. All scores were added to create a composite radiological score with a maximum of six, representing radiological severity.

After radiograph examination, the specimens from the bone defect sites were fixed with 10% paraformaldehyde, decalcified with sodium formate and embedded with paraffin. Cross-sections of bone (5 mm thickness) were stained with H&E and then examined under a light microscope. Slides were randomized and scored by an independent pathologist. Each slide was scored using the method described by Smeltzer et al[25] to rate signs of infection. This score consists of four categories of investigation: acute intraosseous inflammation; chronic intraosseous inflammation; periosteal inflammation; and bone necrosis. A numerical score was assigned to each variable and all scores were added to create a composite histopathologic score with a maximum of 16, representing histopathologic severity.

Statistics. All data were reported as means ± SD unless otherwise stated. A paired *t*-test (when the data had equal variance) and a non-parametric *t*-test (when the data had unequal variance) were performed using SPSS software, version 11.0 (IBM, Armonk, New York), and $p < 0.05$ was considered statistically significant.

Results

Characterisation of vancomycin-loaded composite scaffolds. Figure 1 shows the electron microscopy structure of the composite scaffolds in the inorganic phase. The prepared gelatin/β-TCP scaffolds exhibited a homogeneously interconnected 3D porous structure. Moreover, the β-TCP granules presented uniform distribution on the walls of the composite scaffold. Figure 2 lists the mean diameters of the pores and porosity. The pore size of different scaffolds was not affected by the presence of β-TCP granules. However, the β-TCP granules could modify the structure of composite scaffolds and improve the porosity and interconnection. The porosity and interconnection were significantly increased in G-TCP1 and G-TCP3

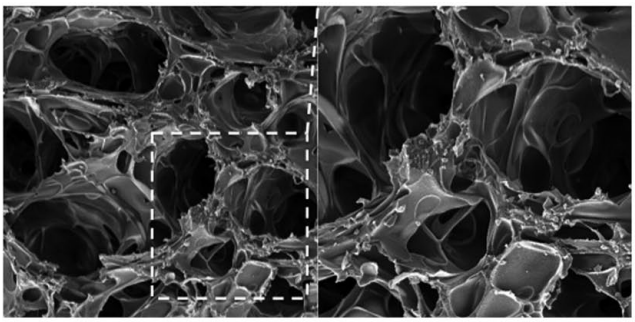

Fig. 1a

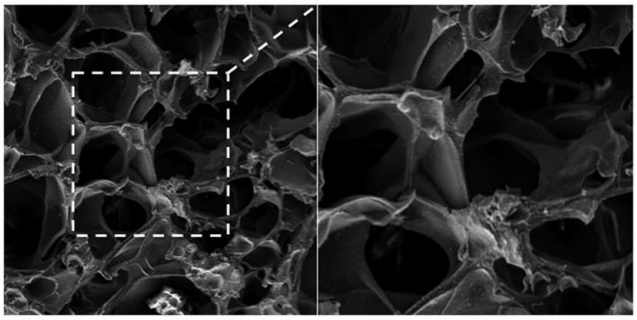

Fig. 1b

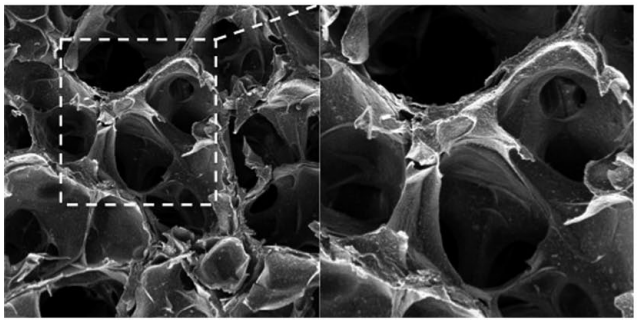

Fig. 1c

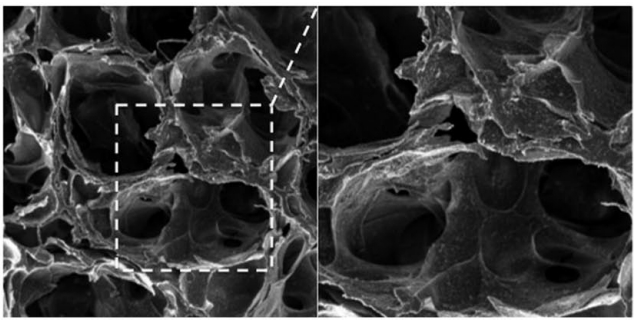

Fig. 1d

The prepared gelatin/β-tricalcium phosphate (β-TCP) scaffolds exhibited a homogeneously interconnected 3D porous structure. The β-TCP granules presented uniform distribution on the walls of G-TCP1, G-TCP3 and G-TCP5 composite scaffolds. a) G-TCP0 scaffold; b) G-TCP1 scaffold; c): G-TCP3 scaffold; d) G-TCP5 scaffold. Images on the right hand side are the enlarged scale of the view on the left.

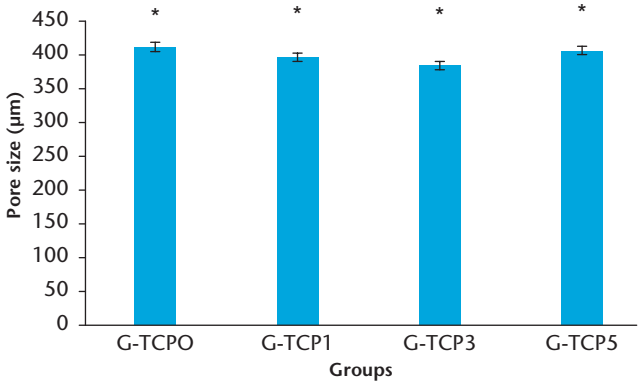

Fig. 2a

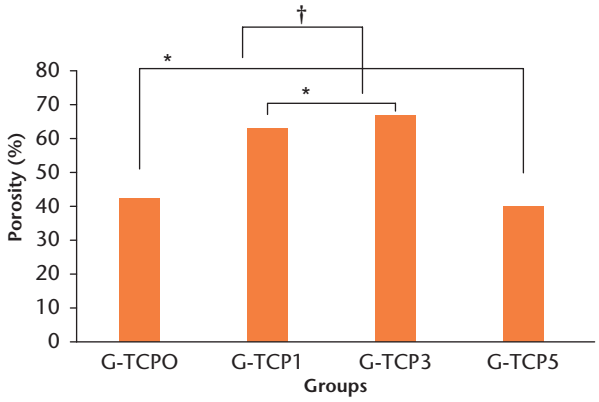

Fig. 2b

The pore size and porosity of the gelatin/β-tricalcium phosphate (β-TCP) composite scaffolds. a: The pore size of different scaffolds was not affected by the presence of β-TCP granules. (*There were no significant differences among the four different scaffolds $p > 0.05$, paired *t*-test). b: The β-TCP granules could improve the porosity of the composite scaffolds. The porosity was significantly increased in G-TCP1 and G-TCP3 scaffolds compared with the pure gelatin scaffold. In contrast, extremely high content of β-TCP granules would decrease the porosity. Moreover, the porosity was significantly decreased in the G-TCP5 scaffold (*there were no significant differences between G-TCP0 and G-TCP5 and between G-TCP1 and G-TCP3; † The porosity of G-TCP1 and G-TCP3 was significantly increased compared with that of G-TCP0 and G-TCP5.

scaffolds compared with the pure gelatin scaffold. In contrast, extremely high content of β-TCP granules decreased the porosity and interconnection. In addition, the porosity and interconnection were significantly decreased in the G-TCP5 scaffold.

The release profile and antibacterial properties. Figure 3 shows the release profiles of vancomycin-loaded composite scaffolds. The G-TCP0 scaffold exhibited the longest duration of vancomycin release with its release duration reaching 56 days. With the increased content of β-TCP granules, the release duration was significantly shortened. Compared with the G-TCP5 scaffold, the composite scaffolds of G-TCP1 and G-TCP3 revealed a slower release of the drug, with the total amount of the drug being released within 42 days. However, the complete release of vancomycin was achieved from the G-TCP5 composite scaffold within 21 days.

Table I shows the inhibition zones of tissue homogenates in different batches of vancomycin-loaded composite scaffolds at different timepoints after implantation.

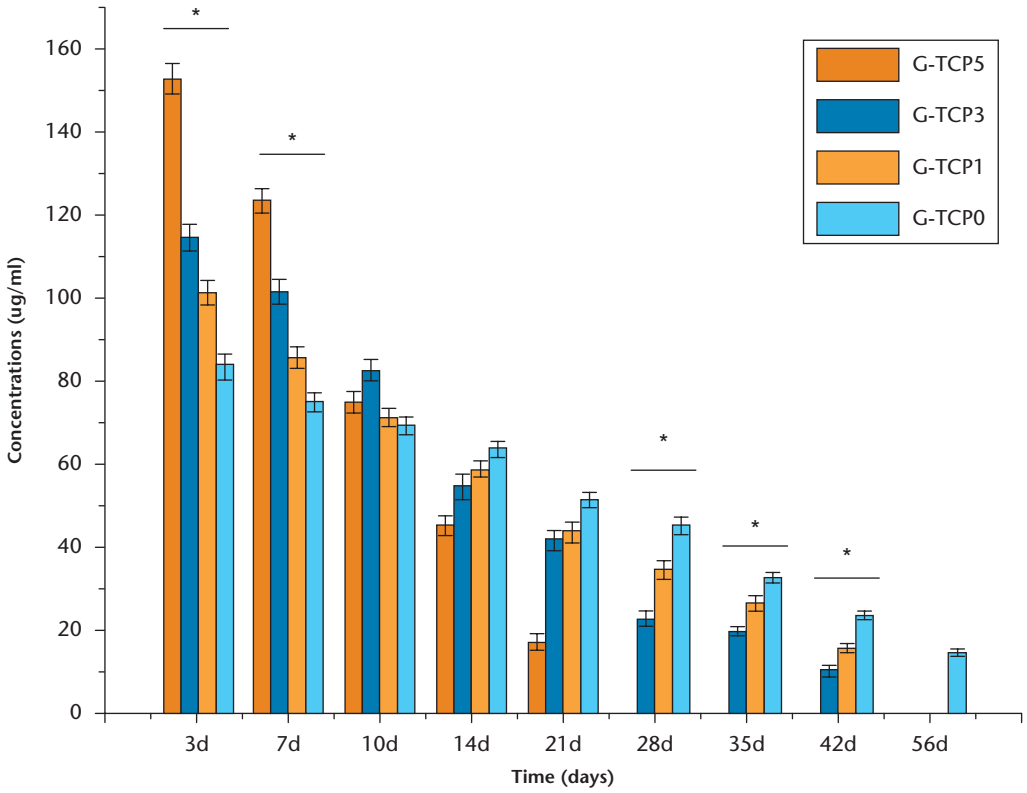

Fig. 3

The release profiles of vancomycin-loaded composite scaffolds with different amounts of β-tricalcium phosphate granules (*Significant differences among the four groups, $p < 0.05$, non-parametric *t*-test).

Table I. The inhibition zones of tissue homogenates in different batches of vancomycin-loaded composite scaffolds at different timepoints after implantation (mm)

Groups	The diameter of inhibition zone at different timepoints after implantation.								
	3 days	**7 days**	**10 days**	**14 days**	**21 days**	**28 days**	**35 days**	**42 days**	**56 days**
G-TCP0 (SD)	10.6 (1.2)*	9.3 (0.5)*	8.1 (0.7)†	7.5 (0.4)†	6.1 (0.3)‡	5.7 (0.4)*	5.2 (0.5)*	4.6 (0.3)*	2.9 (0.2)
G-TCP1 (SD)	12.4 (0.6)*	11.3 (1.1)*	8.3 (0.6)†	6.7 (0.6)†	5.6 (0.4)‡	5.1 (0.6)*	4.7 (0.1)*	3.0 (0.1)*	0
G-TCP3 (SD)	14.5 (0.8)*	12.7 (0.9)*	10.1 (0.4)†	6.3 (0.8)†	5.2 (0.3)‡	4.6 (0.3)*	3.7 (0.2)*	2.6 (0.2)*	0
G-TCP5 (SD)	17.3 (1.1)*	15.1 (0.7)*	9.1 (1.1)†	5.9 (0.5)†	3.1 (0.2)	0	0	0	0

*There were significant differences among the different composite scaffolds at each timepoint
†There were no significant differences among the different composite scaffolds at each timepoint
‡Significant differences were observed compared with the G-TCP5 group
A paired *t*-test was used for the statistical tests

The released vancomycin from the composite scaffolds was bioactive. No effective inhibition zones formed for the tissue homogenate of G-TCP5 after four weeks of implantation.

Biocompatibility. Two weeks after implantation, the gross view of the implanted scaffolds in each group showed that the scaffolds maintained their structures, and they were surrounded by thin fibrous capsules containing vascular vessels without signs of inflammation, such as oedema. Figure 4 shows representative H&E-stained histological sections of vancomycin-loaded composite scaffolds harvested after two weeks of implantation. At this stage, the composite scaffolds maintained their intact interconnecting porous structures. The G-TCP0 scaffold showed no invading host cells inside the implants and only macrophages and host cells were found around the implants. In contrast, the G-TCP1, G-TCP3 and G-TCP5 scaffolds showed prominent infiltration and ingrowth of macrophages and host cells. Figure 4 offers typical histological sections after four weeks of implantation. G-TCP0 and G-TCP1 scaffolds maintained their characteristic microstructural morphology and displayed open pore structures. However, the scaffold integrity was worse compared with those after two weeks of implantation, especially for the G-TCP3 and G-TCP5 scaffolds. After eight weeks of implantation (Fig. 4), the G-TCP0 and G-TCP1 scaffolds still maintained their structures. Only small traces of the G-TCP3 scaffold could be seen,

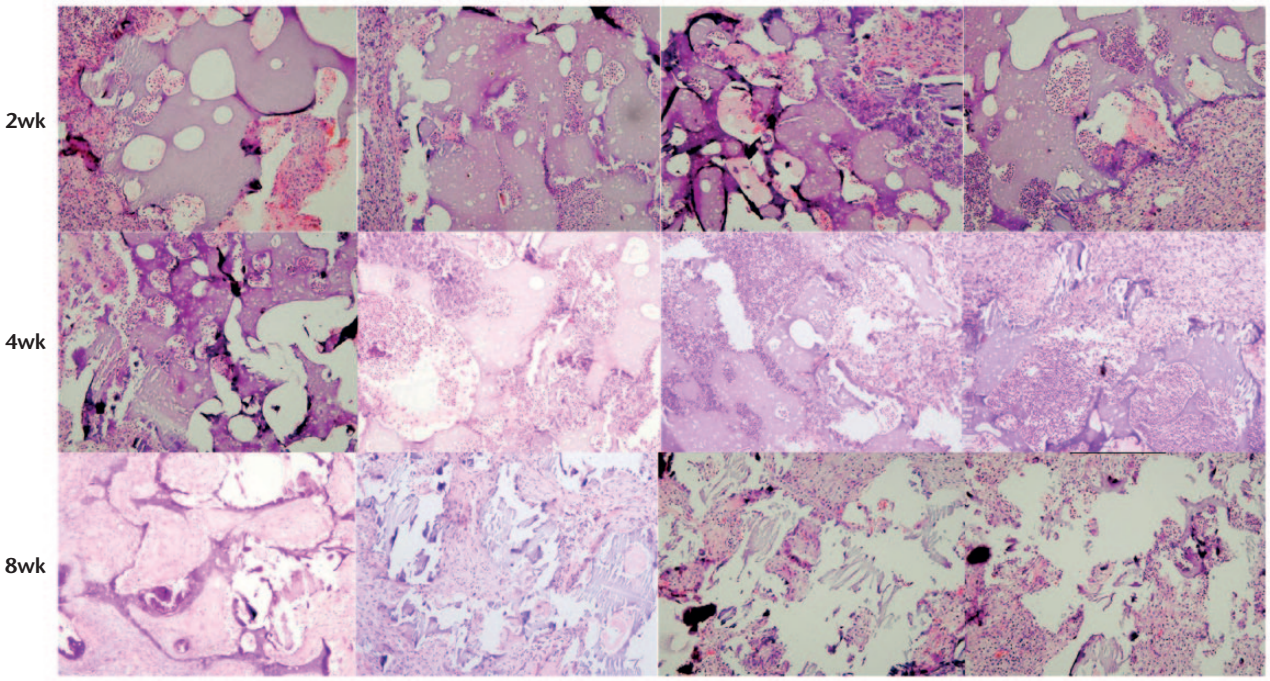

Fig. 4

Haematoxylin and eosin-stained histological sections of vancomycin-loaded composite scaffolds harvested at two weeks, four weeks and eight weeks after implantation. Left to right: G-TCP 0, 1, 3, and 5, respectively.

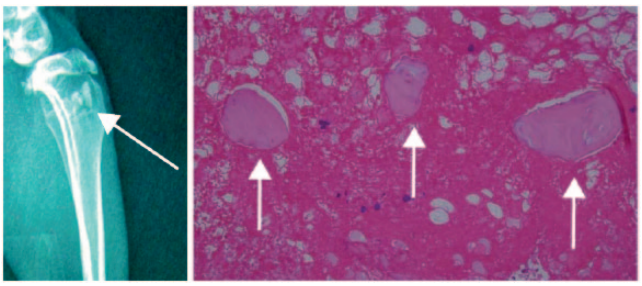

Fig. 5a Fig. 5b

a) Typical radiological evidence of chronic osteomyelitis: reduced bone density; dead bone; subperiosteal abscesses; and new periosteal bone formation (white arrow: sequestrum formation). b) The haematoxylin and eosin staining showed a large number of clearly visible inflammatory cells, interstitial haemorrhage and bone sequestrum formation (white arrow).

however, the G-TCP5 scaffold could not be found. The histological staining (Fig. 4) showed that all of the composite scaffolds had disintegrated with varying degrees of degradation. The G-TCP5 scaffold was almost completely degraded and the cellular infiltration was clearly decreased. A small number of residual scaffold could be seen in the G-TCP3 scaffold, and the residual scaffold were surrounded by giant cells. The G-TCP0 and G-TCP1 scaffolds were partly degraded, and the host cells and several macrophages were observed within the pores of the composite scaffolds.

Osteomyelitis model. No animals died during the experiment. Local below-knee swelling and erythema were observed in all animals under physical examination at five days to seven days after the modelling operation. After ten days to 14 days, the wound formed fistulas and had discharge. Three weeks after the osteomyelitis induction, the right hind leg of all of the rabbits showed the typical radiological evidence of chronic osteomyelitis with the following findings: reduced bone density; dead bone; subperiosteal abscess; and formation of new periosteal bone (Fig. 5a). We confirmed that an animal model of chronic osteomyelitis was successfully established as described by Norden.[24]

Three rabbits were randomly selected and sacrificed to evaluate the presence of osteomyelitis by pathological H&E staining. Figure 5b presents many visible inflammatory cells, interstitial haemorrhage and bone sequestrum formation.

Treatment of osteomyelitis defects in rabbits. No animal died during the treatment. At different postoperative timepoints after the debridement and implantation of vancomycin-loaded composite scaffolds, radiographic and histological examination were used to evaluate the presence of bone lesion changes, degradation and absorption of the implant material and new bone formation.

The radiological results of animals in the control group showed mild osteolysis after four weeks post debridement, and it became more obvious after eight weeks post debridement, showing increases in osteolytic lesions, development of periosteal reactions, new bone formation and sequestral bone formation. In the G-TCP0 group, radiological signs of infection were nearly absent four weeks after debridement and infections were cured after

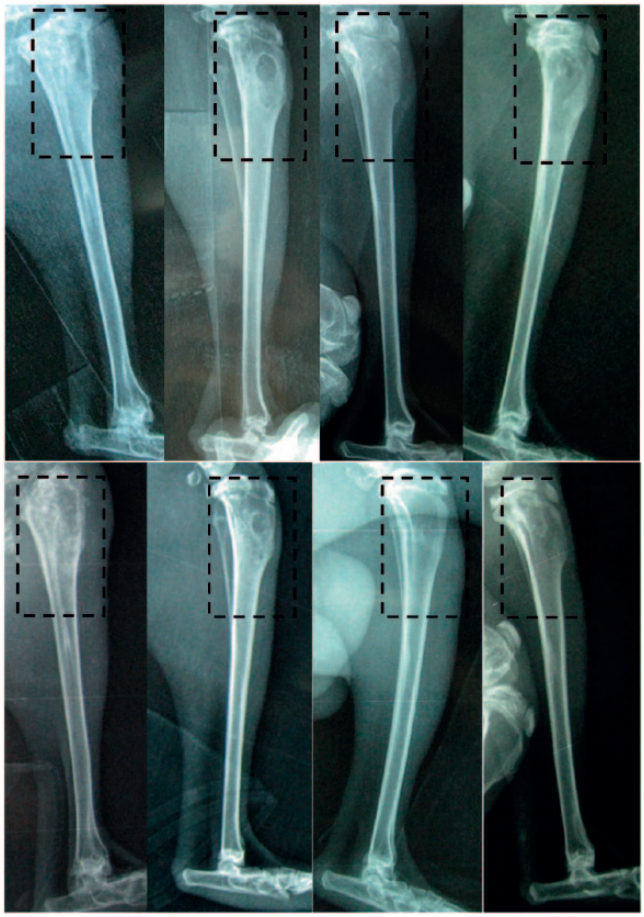

Fig. 6

The radiographic results of animals in the (left to right) control, G-TCP0, G-TCP1 and G-TCP3 groups at four weeks and eight weeks after implantation. top) Four weeks after implantation; bottom) eight weeks after implantation.

eight weeks. However, no bone formation was observed in the defect sites at any timepoint. In the G-TCP1 and G-TCP3 groups, no radiological signs of osteomyelitis were observed and the shape of the proximal tibia was restored to its normal structure after four weeks and eight weeks post debridement and scaffold implantation. In the G-TCP1 group, no bone formed after four weeks and the defects were partially repaired after eight weeks. However, in the G-TCP3 group, some callus formed during the first four weeks and the defects were fully repaired at eight weeks post implantation (Fig. 6).

Quantitative analysis of the radiographs in Table II revealed that there were no significant differences among the radiological scores of the four groups before scaffold implantation, while significant differences were observed after four weeks and eight weeks post implantation. The radiological scores were gradually decreased after surgery for G-TCP0, G-TCP1 and G-TCP3 groups. The control group had significantly higher mean scores compared with the other groups ($p < 0.05$, paired *t*-test). The G-TCP3 group had the best radiological scores after implantation among the four groups. At eight weeks after implantation, the mean scores for the control, G-TCP0, G-TCP1 and G-TCP3 groups were 5.78 (SD 0.13), 2.95 (SD 0.11), 2.46 (SD 0.06) and 0.79 (SD 0.08), respectively. These scores were significantly different ($p < 0.05$, paired *t*-test).

Haematoxylin and eosin histological analysis showed that many inflammatory cells were observed, accompanied by the emergence of tissue necrosis, bone structure destruction and sequestrum formation in the control group after four weeks and eight weeks post debridement. In the G-TCP0 group, inflammatory cells were not observed and a small amount of implant material was degraded and absorbed after four weeks post implantation. After eight weeks post implantation, a large amount of material was clearly visible and no new bone had formed. After four weeks post implantation, no signs of inflammation were found in the G-TCP1 group, some materials were degraded and no new bone had formed. However, after eight weeks post implantation, only a small amount of material was visible and some islands of new trabecular bone had formed. In the G-TCP3 group, no evidence of infection was found after four weeks post implantation, a large amount of material was degraded and some new bone had formed. No material was visible after eight weeks post implantation and a large amount of new bone had formed (Fig. 7). The histopathological scores in the G-TCP0, G-TCP1 and G-TCP3 groups decreased with time and these groups could be ranked in a descending order based on histopathologic severity as follows: G-TCP0 > G-TCP1 > G-TCP3 ($p < 0.05$, paired *t*-test), showing that the best implantation effect was observed in the G-TCP3 group. The histopathological score in the control group was increased with time, and was significantly higher than those of the other groups at each timepoint ($p < 0.05$, paired *t*-test) (Table II).

Discussion

The treatment of infected bone defects remains a clinical challenge because infected bone defects have poor self-healing ability due to the limited blood supply in the infected area. Conventional treatments include drainage, extensive debridement of all necrotic tissues, elimination of dead spaces, adequate soft-tissue coverage and systemic administration of antibiotics for four to six weeks.[26] However, systematic administration of antibiotics yields a limited success rate, which is mainly attributed to the limited blood supply and the formation of a bacteria biofilm that can prevent the infected area from acquiring sufficient antibiotics.[27]

Currently, the standard treatment mainly includes a combination of surgical intervention and administration of an effective local antibiotic therapy. The incorporation of antibiotics into PMMA was originally developed by Buchholz et al.[5] Antibiotic-impregnated PMMA beads provide a high local concentration of the drug and have the ability to fill the bone defects. However, PMMA beads

Table II. Mean radiological and histopathologic scores of the four groups

Groups	Radiological score			Histopathologic score	
	Before treatment	Four wks after treatment	Eight wks after treatment	Four wks after treatment	Eight wks after treatment
Control group (SD)	4.33 (0.23)	5.32 (0.13)	5.78 (0.13)	7.79 (0.15)‡	9.98 (0.23)§
G-TCP0 group (SD)	4.12 (0.14)	3.77 (0.05)*	2.95 (0.11)†	5.45 (0.12)‡	4.23 (0.11)§
G-TCP1 group (SD)	4.27 (0.22)	3.44 (0.09)*	2.46 (0.06)†	4.99 (0.09)‡	3.67 (0.10)§
G-TCP3 group (SD)	4.32 (0.17)	2.37 (0.12)*	0.79 (0.08)†	3.97 (0.13)‡	2.73 (0.09)§

*Significant differences were observed compared with the control group and significant differences were observed among the groups of G-TCP0, G-TCP1 and G-TCP3 ($p < 0.05$)
†Significant differences were observed compared with the control group, and significant differences were observed among the groups of G-TCP0, G-TCP1 and G-TCP3. Significant differences were also observed between eight weeks and four weeks after treatment ($p < 0.05$)
‡Significant differences were observed among the control group, G-TCP0 group, G-TCP1 group and G-TCP3 group ($p < 0.05$)
§Significant differences were observed compared with that of four weeks after treatment ($p < 0.05$), and significant differences were observed among the control group, G-TCP0 group, G-TCP1 group and G-TCP3 group ($p < 0.05$)
A paired *t*-test was used for all p-values

are non-biodegradable, therefore leading to secondary damage to the patient. Furthermore, the major drawbacks of PMMA are its poor binding ability to bone tissue which hampers its biological function.[28] Another disadvantage for using PMMA as the antibiotic carrier is the incomplete release,[29] and the majority of the antibiotics may be retained within the PMMA matrix, sometimes as much as 90% of the total load.[30,31] In contrast, β-TCP ceramic and gelatin are biodegradable, and the gelatin/β-TCP composite scaffold has been proven to be degradable over time and can be replaced by new bone.[13,32] In the current study, we also observed that the G-TCP5 scaffold was almost completely degraded after eight weeks of implantation, and other scaffolds were also degraded to varying degrees (Fig. 4). After complete degradation, vancomycin would be completely released. In our previous study,[17] we have demonstrated that the process of scaffold preparation does not result in detectable changes in the chemical structure of vancomycin. Moreover, the vancomycin released from the composite scaffold should be bioactive, and, in the current study, the K-B disc diffusion test was applied to detect the concentration of released vancomycin and confirm its bioactivity. Table I illustrates inhibition zones of tissue homogenates in different batches of vancomycin-loaded composite scaffolds at different timepoints after implantation. Consequently, the release of vancomycin from the composite scaffolds was completed and still bioactive.

Ideally, it would be best to treat infected bone defects by simultaneously controlling infection and repairing the bone defect. Therefore, biomaterials with capabilities of both bone regeneration and infection control are urgently needed. In general, carriers for local antibiotic delivery should provide the requisite antibiotic delivery rate in the treatment of osteomyelitis, and they should be osteoconductive to enhance bone regeneration after the infection is cured and have the requisite mechanical strength to support physiological loads.[33]

On the one hand, scaffolds for osteogenesis should mimic bone morphology, structure and function to optimize integration into surrounding tissues. Bone is a complex material composed of calcium phosphate deposited within an organic matrix, while the organic matrix is mainly type I collagen. Gelatin is obtained by degradation of collagen and it can be completely resorbable as well as having excellent biocompatibility.[34] The combination of calcium phosphate ceramics with gelatin is of great interest for bone tissue repair because such a combination displays biological characteristics that are similar to those of human bone.[35] Pores are necessary for bone tissue formation because they allow migration and proliferation of osteoblasts and mesenchymal cells, as well as vascularization.[36] The porosity and pore size are important morphological properties of a biomaterial scaffold for bone regeneration. High porosity and large pores enhance bone growth and osseointegration.[37] Studies have shown better osteogenesis for implants with pores > 300 μm.[38] Relatively larger pores favour direct osteogenesis, since they allow vascularization and high oxygenation. In our study, the gelatin/β-TCP composite scaffold showed a homogeneously interconnected porous structure. The pore size varied from 380 μm to 410 μm in different scaffolds and was not affected by the presence of β-TCP granules. The homogeneous porous structure and large pore size facilitated migration and proliferation of osteoblasts and mesenchymal cells, as well as vascularization. However, the presence of β-TCP granules in the composite scaffolds affected the porosity and interconnection. The porosity and interconnection were significantly increased in G-TCP1 and G-TCP3 scaffolds compared with the pure gelatin scaffold. In contrast, an extremely high content of β-TCP granules would decrease the porosity and interconnection. Previous studies have shown that the gelatin/β-TCP composite scaffold improves osteoconduction after the incorporation of β-TCP. Moreover, the composite scaffold can be progressively replaced by newly formed bone *in vivo*. It is suitable for bone tissue engineering, resulting in enhanced bone repair.[32,39]

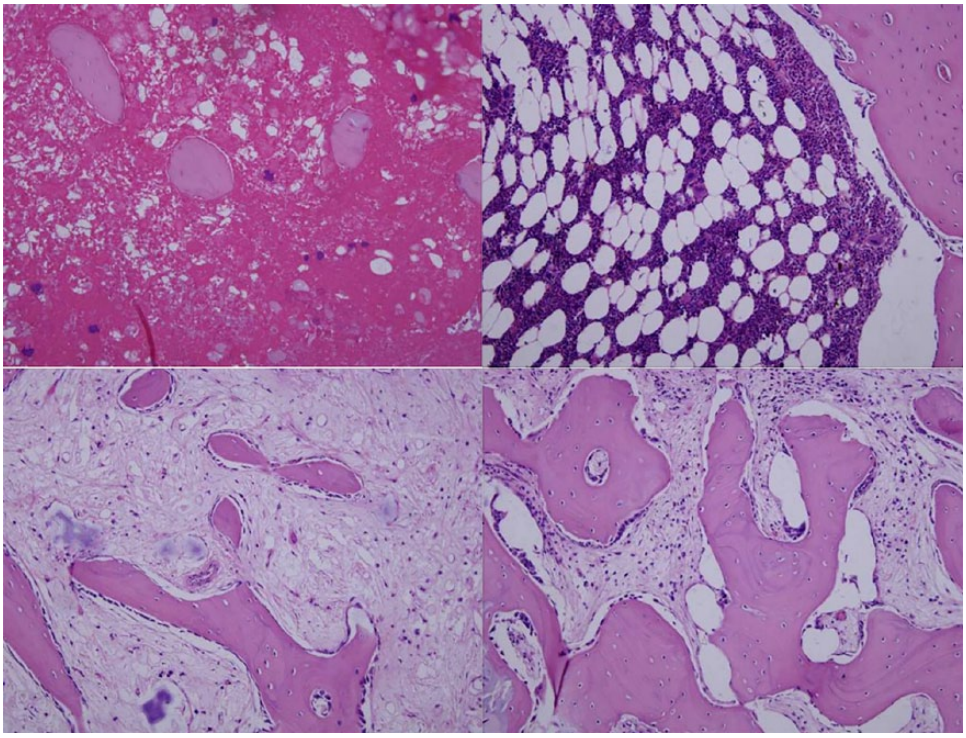

Fig. 7

Histological observation for the repair of osteomyelitis defects in different groups at eight weeks after implantation. (Hematoxylin-eosin stain × 100) Control group (top left): many inflammatory cells were observed, accompanied by sequestrum formation. G-TCP0 group (top right): most of the composite scaffold was clearly visible and no new bone had formed. G-TCP1 group (bottom left): only small amount of material was visible and some islands of new trabecular bone had formed. G-TCP3 group (bottom right): the composite scaffold was completely degraded and a large amount of new bone had formed.

On the other hand, carriers for local antibiotic delivery should provide the requisite antibiotic delivery rate in the treatment of osteomyelitis. Sustained delivery of vancomycin can be achieved through mechanisms of diffusion and matrix degradation. At the early stage after implantation, diffusion is the predominant release mechanism of vancomycin from the crosslinked gelatin matrix. In the later period, the vancomycin released from the crosslinked gelatin matrix is mainly attributed to the biodegradation process.[40,41] Consequently, in the composite scaffolds, the crosslinked gelatin matrix is a key determinant of the controlled release of vancomycin. Using consistent weights of the composite scaffolds, the content of gelatin was decreased as β-TCP was increased. Moreover, gelatin serves as a binding material between incorporated β-TCP particles to maintain the structure of gelatin/β-TCP sponges. Therefore, the sponges with higher β-TCP contents collapse and deform easily under wet and proteolytic conditions due to the faster loss of gelatin mass by degradation.[13] In the composite scaffold of G-TCP5, the amount of gelatin matrix was relatively low compared with other composite scaffolds. More vancomycin was superficially absorbed onto the outermost surface and it revealed a large initial burst release. Due to the lowest content of gelatin, the G-TCP5 composite scaffold deformed quickly and vancomycin could be completely released from the G-TCP5 scaffold within only three weeks. In contrast, vancomycin was released from the G-TCP0 scaffold within eight weeks with a reduction of initial burst release due to its high content of gelatin.

The *in vivo* degradation in the current study confirmed the release profile of the composite porous scaffold. We found that the implanted scaffolds in each group maintained their shapes and intact interconnecting porous structures at two weeks after implantation. The G-TCP0 scaffold showed no invading host cells inside the implants. In contrast, the G-TCP1, G-TCP3 and G-TCP5 scaffolds showed prominent infiltration and ingrowth of host cells. Moreover, G-TCP0 and G-TCP1 scaffolds maintained their characteristic morphology and displayed open pore structures at four weeks after implantation, but the scaffold integrity was weakened, especially for the G-TCP3 and G-TCP5 scaffolds. In addition, the G-TCP0 and G-TCP1 scaffolds still maintained their shape at eight weeks after implantation and only a small trace of the G-TCP3 scaffold could be seen, while the G-TCP5 scaffold became completely undetectable.

In the present chronic osteomyelitis model, the vancomycin-loaded gelatin/β-TCP composite porous scaffolds were implanted for assessment of infection control and bone defect repair. The *in vivo* release profile and degradation showed that the G-TCP5 scaffold could only release vancomycin for three weeks and then it was quickly degraded. The vancomycin-loaded

G-TCP5 scaffold could not fulfil the requirement of clinical treatment for chronic osteomyelitis and infected defects. Moreover, we also investigated the therapeutic efficacy for the treatment of osteomyelitis in rabbits. The radiographic and histological evaluation all showed that the infections were eliminated in the G-TCP0, G-TCP1 and G-TCP3 scaffolds at eight weeks after implantation. However, the infection recurred in the control group since no vancomycin-loaded scaffolds were implanted. For the bone defect repair, the G-TCP0 group showed no repair on the radiograph and no new bone formation in the histological investigation at eight weeks after implantation. In the G-TCP1 group, only a small amount of new bone formed and the defect was partly repaired. The radiograph showed that the defect was completely repaired in the G-TCP3 group at eight weeks after implantation and a large amount of new bone formation could be detected in the H&E-stained histological slides. This might be attributed to the presence of β-TCP granules, which improved the osteoconduction of the porous scaffolds and enhanced bone regeneration after the infection was cured.

The vancomycin-loaded gelatin/β-TCP composite scaffolds prepared in this study achieved the desired local therapeutic drug levels over an extended duration. The composite scaffold consisting of gelatin and 30% β-TCP granules showed optimal porosity, interconnection and controlled release performances. It exhibited good performances in infection control and bone defect repair in the chronic MRSA osteomyelitis model. Vancomycin-loaded gelatin/β-TCP composite scaffolds could potentially be used in the clinical treatment of osteomyelitis defects.

References

1. **Lazzarini L, Mader JT, Calhoun JH.** Osteomyelitis in long bones. *J Bone Joint Surg [Am]* 2004;86-A:2305-2318.
2. **Lew DP, Waldvogel FA.** Osteomyelitis. *N Engl J Med* 1997;336:999-1007.
3. **Morris R, Hossain M, Evans A, Pallister I.** Induced membrane technique for treating tibial defects gives mixed results. *Bone Joint J* 2017;99-B:680-685.
4. **Hanssen AD, Spangehl MJ.** Practical applications of antibiotic-loaded bone cement for treatment of infected joint replacements. *Clin Orthop Relat Res* 2004;427:79-85.
5. **Buchholz HW, Elson RA, Engelbrecht E, et al.** Management of deep infection of total hip replacement. *J Bone Joint Surg [Br]* 1981;63-B:342-353.
6. **Ristiniemi J, Lakovaara M, Flinkkilä T, Jalovaara P.** Staged method using antibiotic beads and subsequent autografting for large traumatic tibial bone loss: 22 of 23 fractures healed after 5-20 months. *Acta Orthop* 2007;78:520-527.
7. **Gaowa A, Horibe T, Kohno M, et al.** Combination of hybrid peptide with biodegradable gelatin hydrogel for controlled release and enhancement of anti-tumor activity in vivo. *J Control Release* 2014;176:1-7.
8. **Nguyen AH, McKinney J, Miller T, Bongiorno T, McDevitt TC.** Gelatin methacrylate microspheres for controlled growth factor release. *Acta Biomater* 2015;13:101-110.
9. **Santoro M, Tatara AM, Mikos AG.** Gelatin carriers for drug and cell delivery in tissue engineering. *J Control Release* 2014;190:210-218.
10. **Martínez-Vázquez FJ, Cabañas MV, Paris JL, Lozano D, Vallet-Regí M.** Fabrication of novel Si-doped hydroxyapatite/gelatine scaffolds by rapid prototyping for drug delivery and bone regeneration. *Acta Biomater* 2015;15:200-209.
11. **Nouri-Felekori M, Mesgar AS, Mohammadi Z.** Development of composite scaffolds in the system of gelatin– calcium phosphate whiskers/fibrous spherulites for bone tissue engineering. *Ceram Int* 2015;41:6013-6019.
12. **Ho CC, Huang SC, Wei CK, Ding SJ.** In vitro degradation and angiogenesis of the porous calcium silicate–gelatin composite scaffold. *J Mater Chem B Mater Biol Med* 2016;4:505-512.
13. **Takahashi Y, Yamamoto M, Tabata Y.** Osteogenic differentiation of mesenchymal stem cells in biodegradable sponges composed of gelatin and β-tricalcium phosphate. *Biomaterials* 2005;26:3587-3596.
14. **Yaszemski MJ, Payne RG, Hayes WC, Langer R, Mikos AG.** Evolution of bone transplantation: molecular, cellular and tissue strategies to engineer human bone. *Biomaterials* 1996;17:175-185.
15. **Xu M, Zhang X, Meng S, et al.** Enhanced critical size defect repair in rabbit mandible by electrospun gelatin/β-TCP composite nanofibrous membranes. *J Nanomater* 2015;2015:3.
16. **Omata K, Matsuno T, Asano K, et al.** Enhanced bone regeneration by gelatin-β-tricalcium phosphate composites enabling controlled release of bFGF. *J Tissue Eng Regen Med* 2014;8:604-611.
17. **Zhou J, Fang T, Wang Y, Dong J.** The controlled release of vancomycin in gelatin/β-TCP composite scaffolds. *J Biomed Mater Res A* 2012;100:2295-2301.
18. **Panzavolta S, Fini M, Nicoletti A, et al.** Porous composite scaffolds based on gelatin and partially hydrolyzed α-tricalcium phosphate. *Acta Biomater* 2009;5:636-643.
19. **Chen G, Ushida T, Tateishi T.** A biodegradable hybrid sponge nested with collagen microsponges. *J Biomed Mater Res* 2000;51:273-279.
20. **McFarland J.** Nephelometer: an instrument for media used for estimating the number of bacteria in suspensions used for calculating the opsonic index and for vaccines. *J Am Med Assoc* 1907; 14:1176-8.y
21. **Donelli G, Francolini I, Piozzi A, Di Rosa R, Marconi W.** New polymer-antibiotic systems to inhibit bacterial biofilm formation: a suitable approach to prevent central venous catheter-associated infections. *J Chemother* 2002;14:501-507.
22. **Yin Y, Ye F, Cui J, et al.** Preparation and characterization of macroporous chitosan-gelatin/β-tricalcium phosphate composite scaffolds for bone tissue engineering. *J Biomed Mater Res A* 2003;67:844-855.
23. **Jiang JL, Li YF, Fang TL, et al.** Vancomycin-loaded nano-hydroxyapatite pellets to treat MRSA-induced chronic osteomyelitis with bone defect in rabbits. *Inflamm Res* 2012;61:207-215.
24. **Norden CW.** Experimental chronic staphylococcal osteomyelitis in rabbits: treatment with rifampin alone and in combination with other antimicrobial agents. *Rev Infect Dis* 1983;5(Suppl 3):S491-S494.
25. **Smeltzer MS, Thomas JR, Hickmon SG, et al.** Characterization of a rabbit model of staphylococcal osteomyelitis. *J Orthop Res* 1997;15:414-421.
26. **Lindbloom BJ, James ER, McGarvey WC.** Osteomyelitis of the foot and ankle: diagnosis, epidemiology, and treatment. *Foot Ankle Clin* 2014;19:569-588.
27. **Zimmerli W.** Clinical presentation and treatment of orthopaedic implant-associated infection. *J Intern Med* 2014;276:111-119.
28. **Matos AC, Marques CF, Pinto RV, et al.** Novel doped calcium phosphate-PMMA bone cement composites as levofloxacin delivery systems. *Int J Pharm* 2015;490:200-208.
29. **Wendling A, Mar D, Wischmeier N, Anderson D, McIff T.** Combination of modified mixing technique and low frequency ultrasound to control the elution profile of vancomycin-loaded acrylic bone cement. *Bone Joint Res* 2016;5:26-32.
30. **Díez-Peña E, Frutos G, Frutos P, Barrales-Rienda JM.** Gentamicin sulphate release from a modified commercial acrylic surgical radiopaque bone cement. I. Influence of the gentamicin concentration on the release process mechanism. *Chem Pharm Bull (Tokyo)* 2002;50:1201-1208.
31. **van de Belt H, Neut D, Schenk W, et al.** Gentamicin release from polymethylmethacrylate bone cements and Staphylococcus aureus biofilm formation. *Acta Orthop Scand* 2000;71:625-629.
32. **Matsumoto G, Omi Y, Kubota E, et al.** Enhanced regeneration of critical bone defects using a biodegradable gelatin sponge and β-tricalcium phosphate with bone morphogenetic protein-2. *J Biomater Appl* 2009;24:327-342.
33. **Chang W, Colangeli M, Colangeli S, et al.** Adult osteomyelitis: debridement versus debridement plus Osteoset T pellets. *Acta Orthop Belg* 2007;73:238-243.
34. **Bigi A, Panzavolta S, Rubini K.** Relationship between triple-helix content and mechanical properties of gelatin films. *Biomaterials* 2004;25:5675-5680.
35. **Habraken WJEM, Wolke JGC, Jansen JA.** Ceramic composites as matrices and scaffolds for drug delivery in tissue engineering. *Adv Drug Deliv Rev* 2007;59:234-248.
36. **Kuboki Y, Takita H, Kobayashi D, et al.** BMP-induced osteogenesis on the surface of hydroxyapatite with geometrically feasible and nonfeasible structures: topology of osteogenesis. *J Biomed Mater Res* 1998;39:190-199.
37. **Karageorgiou V, Kaplan D.** Porosity of 3D biomaterial scaffolds and osteogenesis. *Biomaterials* 2005;26:5474-5491.

38. Götz HE, Müller M, Emmel A, et al. Effect of surface finish on the osseointegration of laser-treated titanium alloy implants. *Biomaterials* 2004;25:4057-4064.
39. Chen KY, Shyu PC, Dong GC, et al. Reconstruction of calvarial defect using a tricalcium phosphate-oligomeric proanthocyanidins cross-linked gelatin composite. *Biomaterials* 2009;30:1682-1688.
40. Xu J, Xu B, Shou D, Xia X, Hu Y. Preparation and evaluation of vancomycin-loaded N-trimethyl chitosan nanoparticles. *Polymers (Basel)* 2015;7:1850-1870.
41. Gao P, Nie X, Zou M, Shi Y, Cheng G. Recent advances in materials for extended-release antibiotic delivery system. *J Antibiot (Tokyo)* 2011;64:625-634.

Funding Statement
- Grants: National Natural Science Foundation of China (81301577); Shanghai Rising Star Program (15QA1401000); and the Specialized Research Fund for the Doctoral Program of Higher Education (20130071120062).

Author Contribution
- J. Zhou: Carried out experiments, Analysed experimental results, Wrote the paper.
- X. G. Zhou: Carried out experiments, Analysed experimental results, Wrote paper.
- J. W. Wang: Assisted with performing animal experiments.
- H. Zhou: Assisted with analysing results.
- J. Dong: Designed experiments.

- J. Zhou and X.G. Zhou contributed equally to this paper.

Conflicts of Interest Statement
- None declared